Supplementary Materials for

Rabphilin3A Reduces Integrin-Dependent Axonal Growth Cone Signaling to Restrict Regeneration after Spinal Cord Injury

Yuichi Sekine, Ramakrishnan Kannan, Xingxing Wang and Stephen M. Strittmatter

****

This PDF file includes Figs. S1 to S11.

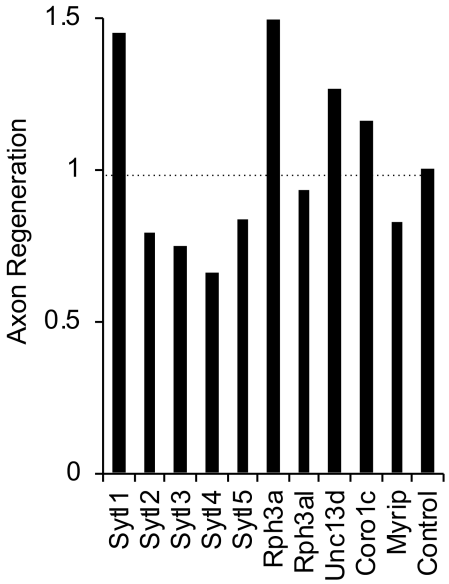

Fig. S1. Axon Regeneration after Rab effector gene knockdown.
The summary of axonal regeneration of Rab effector genes relative to control from full screen results *(21).*

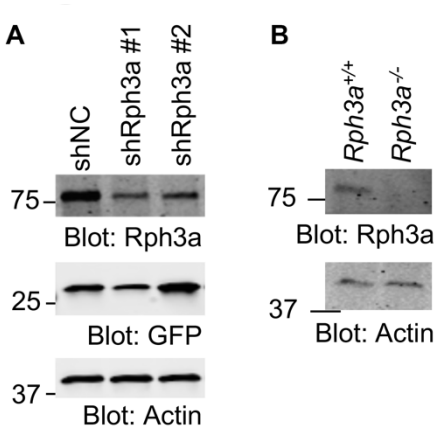

Fig. S2. Rph3a protein levels in cultured cortical neurons.
(A) The lysate from shNC or shRph3a nucleofected neurons was immunoblotted with anti-Rph3a, GFP and Actin antibodies.
(B) The lysate from *Rph3a*$^{+/+}$ or *Rph3a*$^{-/-}$ neurons was immunoblotted with anti-Rph3a and Actin antibodies.

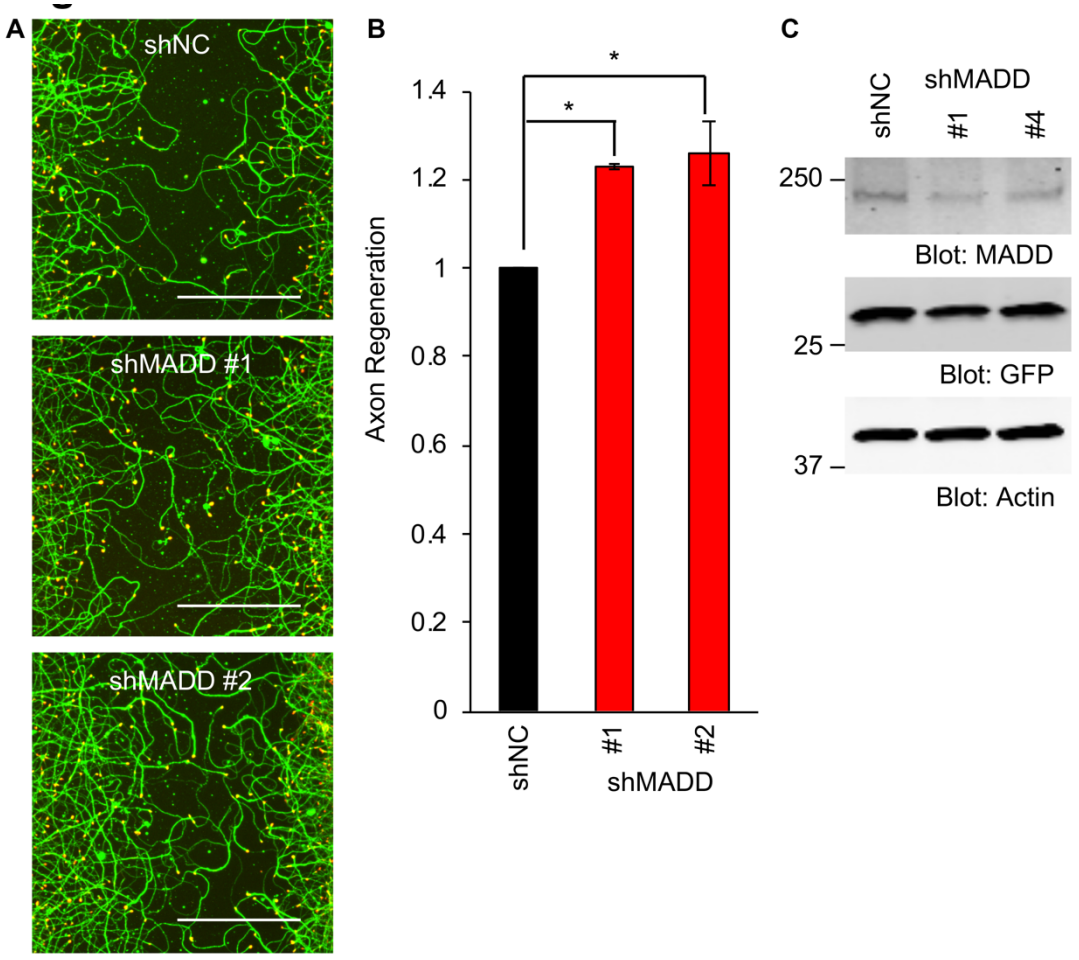

Fig. S3. Suppression of MADD expression enhances axonal regeneration *in vitro*
(A) Representative pictures of regenerated axons nucleofected with shNC, shMADD #1 or #2 in cortical neurons. The microphotographs show ßIII-tubulin (in axons; green) and phalloidin (to stain F-actin; red) to illustrate the growth cones of cortical neurons in the middle of the scraped area. Scale bars represent 200 µm.
(B) The graph shows quantification of axonal regeneration relative to shNC. Mean ± SEM, n=3 biological replicates. *p<0.05, one-way ANOVA followed by Tukey's test.
(C) The lysate from shNC or shMADD nucleofected neurons was immunoblotted with anti-MADD, GFP and Actin antibodies.

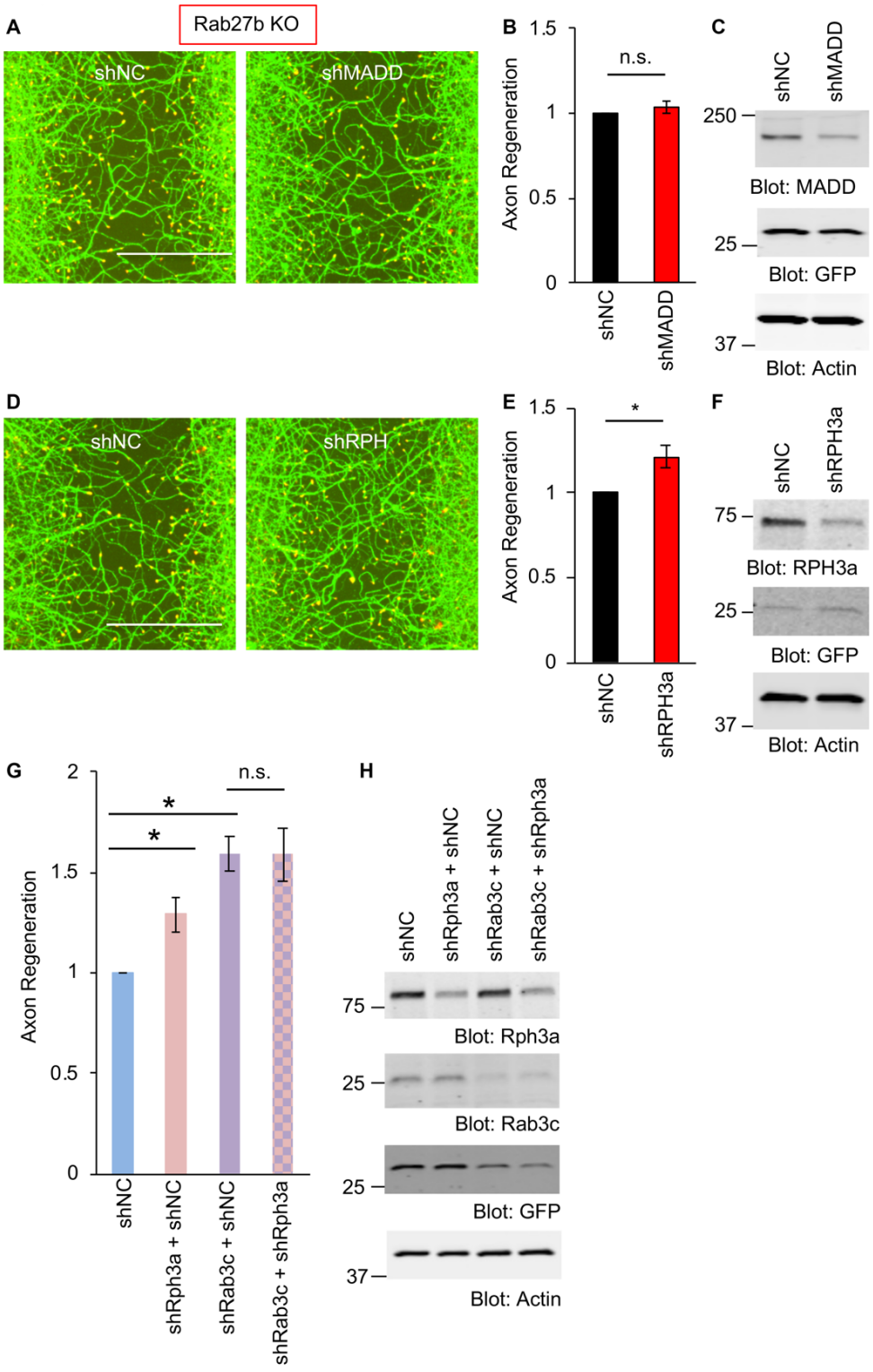

Fig. S4. Effect of MADD, Rph3a and Rab3c expression in *Rab27b*$^{-/-}$ *neuron* on axonal regeneration *in vitro*

(A) Representative pictures of regenerated axons nucleofected with shNC, shMADD in *Rab27b*$^{-/-}$ cortical neurons. The microphotographs show ßIII-tubulin (in axons; green) and phalloidin (to

stain F-actin; red) to illustrate the growth cones of cortical neurons in the middle of the scraped area. Scale bars represent 200 µm.
(B) The graph shows quantification of axonal regeneration relative to shNC. Mean ± SEM, n=8 biological replicates. No significant difference (n.s.), p=0.15, Student *t*-test.
(C) The lysate from shNC or shMADD nucleofected neurons was immunoblotted with anti-MADD, GFP and Actin antibodies.
(D) Representative pictures of regenerated axons nucleofected with shNC, shRph3a in *Rab27b*$^{-/-}$ cortical neurons. The microphotographs show ßIII-tubulin (in axons; green) and phalloidin (to stain F-actin; red) to illustrate the growth cones of cortical neurons in the middle of the scraped area. Scale bars represent 200 µm.
(E) The graph shows quantification of axonal regeneration relative to shNC. Mean ± SEM, n=7 biological replicates. *p<0.05, Student *t*-test.
(F) The lysate from shNC or shRph3a nucleofected neurons was immunoblotted with anti-Roh3a, GFP and Actin antibodies.
(G) *Rab27b*$^{-/-}$ cortical neurons were nucleofected indicated shRNAs and performed scraping assay. The graph shows quantification of axonal regeneration relative to shNC. Mean ± SEM, n=6 biological replicates. *p<0.01, one-way ANOVA followed by Tukey's test. n.s: No significant difference.
(H) The lysate from shNC, shRph3a, shRab3c or shRph3a+shRab3c transfected in *Rab27b*$^{-/-}$ neurons was immunoblotted with anti-Rph3a, Rab3c, GFP and Actin antibodies.

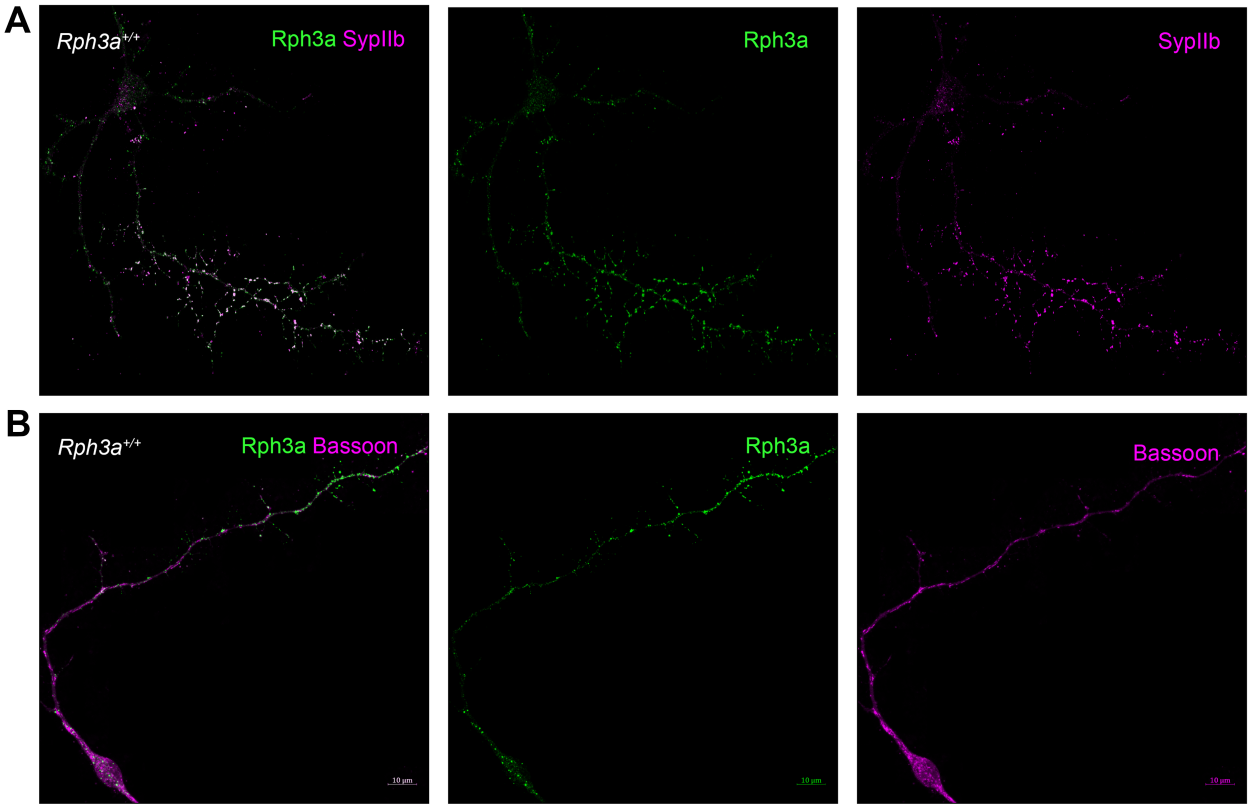

Fig. S5. Rph3a localization with other synaptic vesicle and pre-synaptic proteins
(A and B) Representative Airyscan confocal images of WT and *Rph3a*$^{-/-}$, 7DIV cortical neurons. Immunofluorescence of Rph3a (green) with vesicle membrane marker; Synapsin I (Syp I, magenta in A) and pre-synaptic membrane marker Bassoon (magenta in B) were shown. Scale bar, 10 µm.

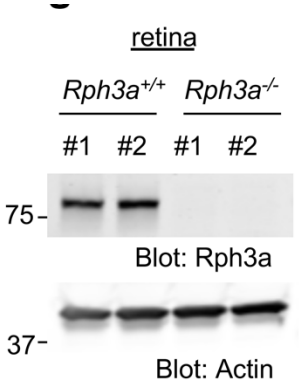

Fig. S6. Expression of Rph3a in the retina
The lysate from *Rph3a*$^{+/+}$ or *Rph3a*$^{-/-}$ retina was immunoblotted with anti-Rph3a and Actin antibodies.

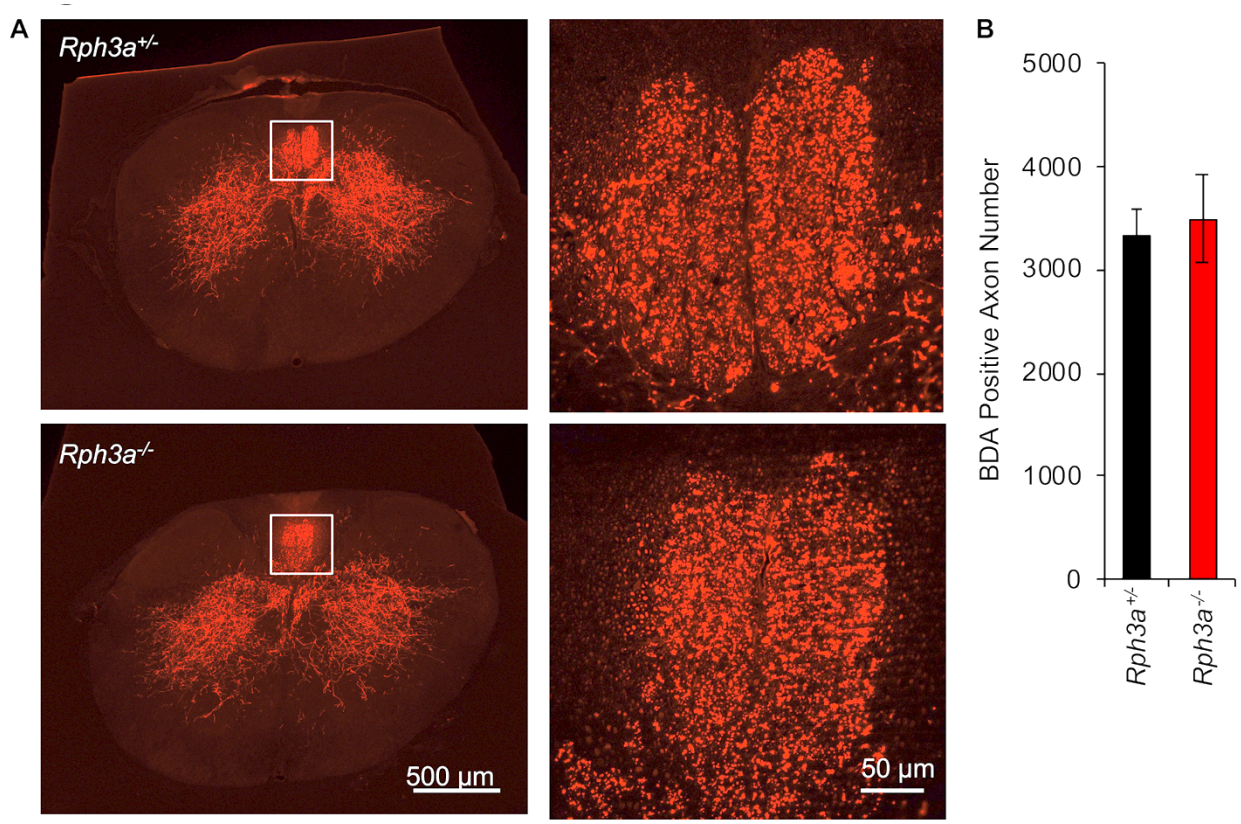

Fig. S7. CST axons of upper cervical cord in injured animals
(A) BDA-labeled CST axons in C1 cervical cord transverse sections from *Rph3a*$^{+/-}$ or *Rph3a*$^{-/-}$ mice. Scale bar represents 500 μm. Right, High-magnification view of white boxes shown in left images. Scale bar represents 100 μm.
(B) Total BDA-positive axon numbers per animal are counted. Mean ± SEM, n=17 *Rph3a*$^{+/-}$ and n=12 *Rph3a*$^{-/-}$. No significant differences between groups with Student's t test.

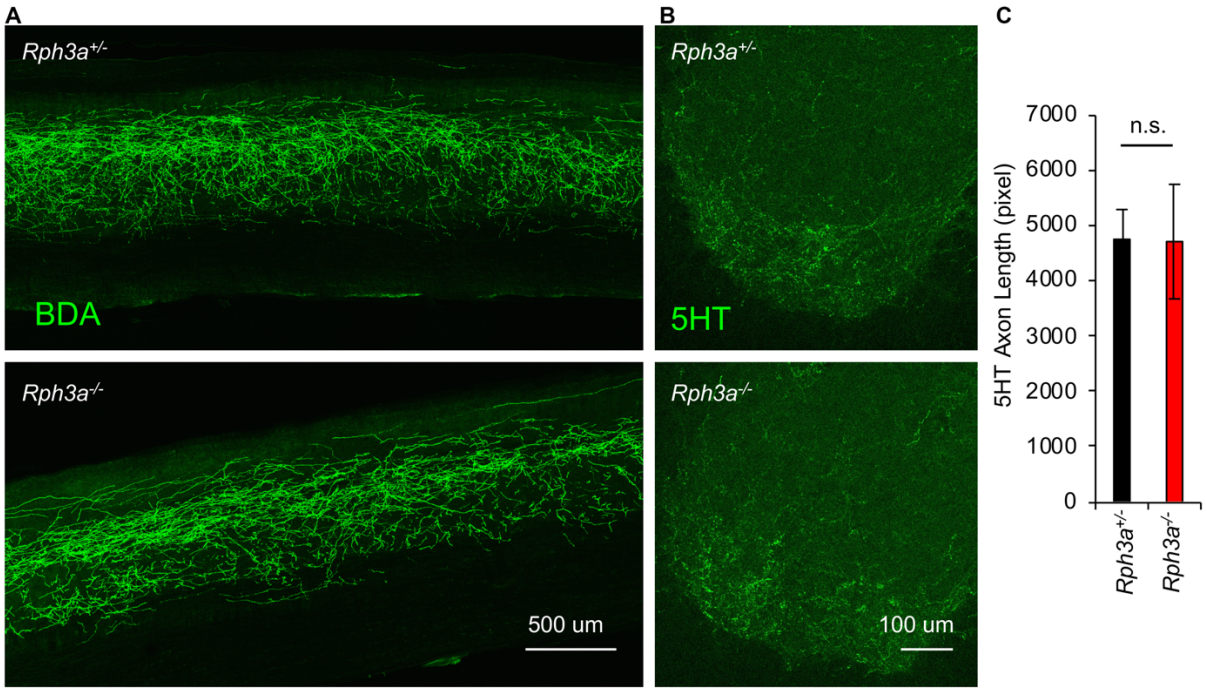

Fig. S8. Comparison of CST and 5HT neurons in uninjured *Rph3a*$^{+/-}$ *and Rph3a*$^{-/-}$ animals.
(A) BDA labeled CST neurons in uninjured *Rph3a*$^{+/-}$ or *Rph3a*$^{-/-}$ mice. Scale bar represents 500 μm.
(B) Serotonergic (5HT+) fiber density in coronal sections of *Rph3a*$^{+/-}$ and *Rph3a*$^{-/-}$ mice. Scale bar represents 100 μm.
(C) Quantification of 5HT-stained neuron length of *Rph3a*$^{+/-}$ and *Rph3a*$^{-/-}$ mice. Mean ± SEM, n=4 *Rph3a*$^{+/-}$ and n=3 *Rph3a*$^{-/-}$. No significant differences between groups by Student's t test.

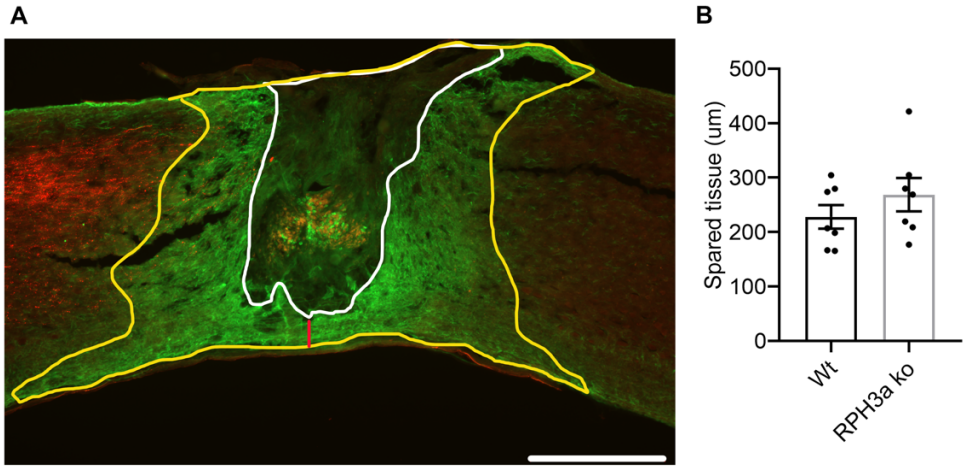

Fig. S9. Spinal Cord Contusion Gliosis is not Altered by Rph3a.
(A) *Rph3a* deletion does not alter scar formation or spared tissue at the site of contusion injury. Representative image of lesion measurement at the site of injury. Section stained with anti-RFP (red) and anti-GFAP (green) antibodies. The area of fibrotic scar is outlined in white and the area of glia reactions is outlined in yellow. The spared tissue is indicated by the red vertical bar. Rostral is to the left and dorsal is up. Scale bar=500 μm.
(B) There is no difference of the extent of spared tissue between the *Rph3a*$^{-/-}$ group and WT group. Data are mean ± SEM; Student's t-test, *p<0.05.
(D) The locomotor BMS scores is plotted as a function of time after SCI. There is a trend of increasing BMS scores at week 10, 12 and 14 post SCI in *Rph3a*$^{-/-}$ mice (red, n=21) compared to control mice (black, n=20, combined 13 heterozygous *Rph3a*$^{-/-}$ plus 7 WT mice) but the differences are not statistically significant different by one-way repeated measure ANOVA. Data are mean ± SEM.

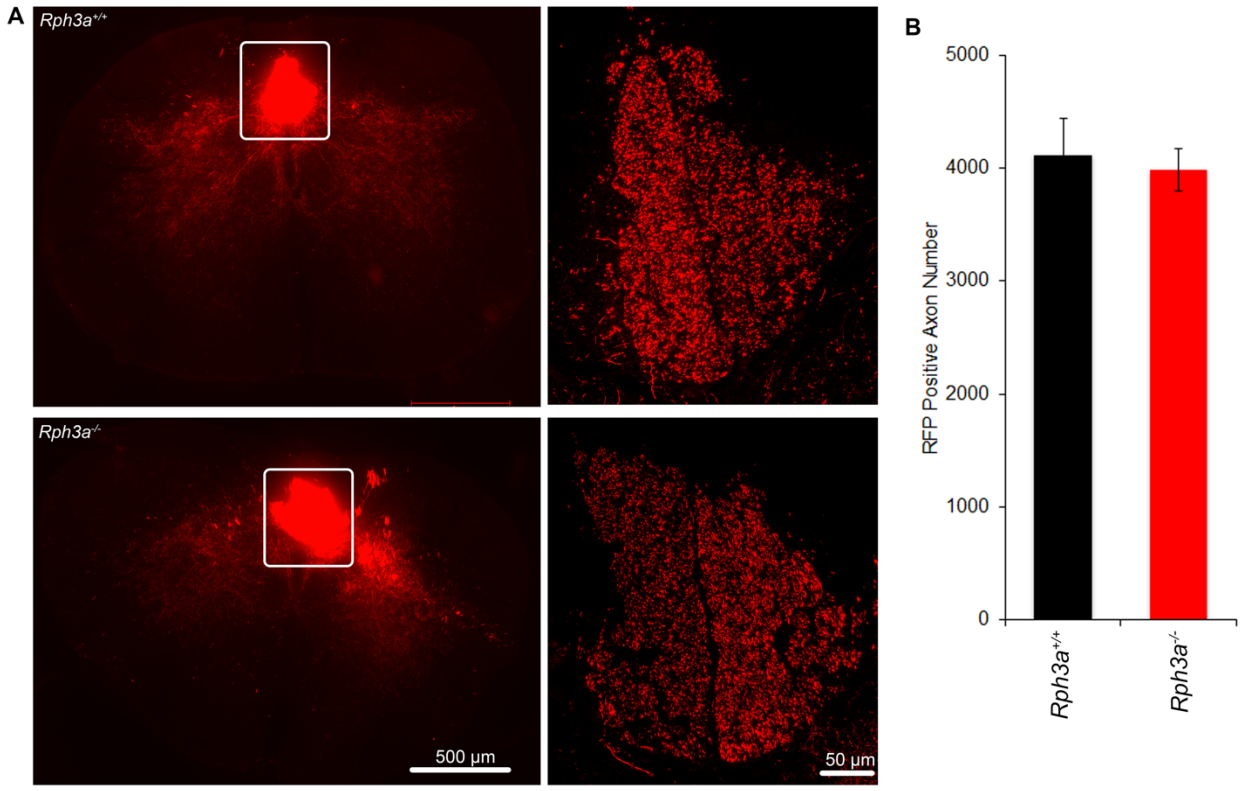

Fig. S10. CST axons of cervical spinal cord in injured animals
(A) RFP-expressing CST neurons in C1 transverse spinal cord sections from *Rph3a*$^{+/+}$ or *Rph3a*$^{-/-}$ mice. Right, High-magnification view of white boxes shown in left images. Scale bars as indicated.
(B) RFP-positive axon numbers are counted. Mean ± SEM, n=7 *Rph*$^{+/+}$ and n=7 *Rph3a*$^{-/-}$. No significant differences between groups with Student's t test.

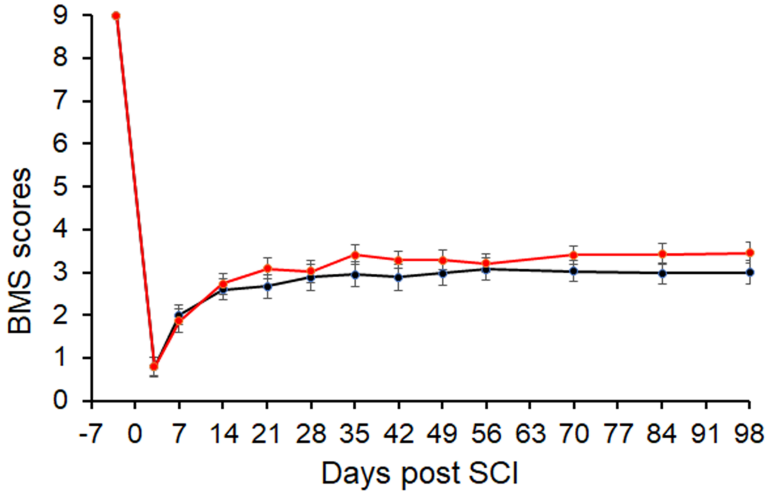

Fig. S11. Locomotor receovery after spinal contusion.
The locomotor BMS scores is plotted as a function of time after SCI. There is a trend of increasing BMS scores at week 10, 12 and 14 post SCI in *Rph3a*$^{-/-}$ mice (red, n=21) compared to control mice (black, n=20, combined 13 heterozygous *Rph3a*$^{-/-}$ plus 7 WT mice) but the differences are not statistically significant different by one-way repeated measure ANOVA. Data are mean ± SEM.